Segmentation, Matching and Estimation of Structure and Motion of Textured Piecewise Planar Surfaces

Sanghoon Sull and *Narendra Ahuja* *
Beckman Institute
University of Illinois, Urbana, IL 61801

Abstract

We present an algorithm which segments and matches the regions and then estimates non-iteratively 3D motion and structure of a moving piecewise planar textured surface from two perspective views. The algorithm has two major steps. The first step is coarse. Here, the local planar nature of the surface is used to obtain polynomial expressions for image plane displacements of features. Using regions as moving features, the image is segmented using Hough transform such that the regions in each segment have the same polynomial coefficients. The values of these coefficients and region properties (e.g., area) are then used to identify region correspondences. In the second step, for each planar surface, the region correspondences are used to compute the corresponding motion parameters and surface orientation in closed form. The second step uses a finer model of motion than the first step. Experimental results are presented for three image pairs.

1 Introduction

Estimation of motion and structure is an important problem in computer vision. There are two major approaches to this problem, which are based on optical flow and feature correspondence. If the problem of feature correspondence can be solved, the feature-based approach is preferred to the optical flow based approach since a straightforward implementation of the latter is highly noise sensitive due to its dependence on spatiotemporal gradients. Features such as points, lines and region contours [1,2,3] are commonly used for the former. Macro features such as lines and contours are less sensitive to noise and are easier to match than points.

There have been several region-based approaches. Kanatani [1] developed a method for computing motion parameters for scenes with known initial structure; his method is based on values of certain integrals Computed on one planar region, under the assumption that the motion is infinitesimal. Kanatani [2] also presented an iterative method for the finite motion case, which treats finite motion in the same way as infinitesimal motion. The solution is obtained iteratively by using the current solution as the initial state for the next iteration. But this method does not always converge. Wu [3] proposed an iterative method based on the optical flow on a contour. It was reported that the method usually converges if the maximal motion is smaller than a threshold related to the contour size.

In this paper, we present an algorithm which segments and matches the regions and then estimates motion and structure parameters of piecewise planar surfaces. We assume that the 3D scene has planar surfaces each of which is textured in the sense that each plane has at least 4 regions. Thus each region boundary is also planar. We use region correspondences instead of commonly used point features because regions are more robust features than points: being smaller in number, they are easier to match; they have more measurable properties than points (which are characterized only by their positions); and, in some images it is very difficult to extract point features (e.g., See Fig. 1.(a)).

In our algorithm, the displacement (flow) field of the image plane is approximated by second order polynomials which are obtained from the basic motion equations and the planar nature of surfaces. Then, by using the first order flow coefficients as the parameters of Hough transform, the algorithm partitions the set of regions into segments (groups) where each segment exhibits rigid planar motion. Then, for a given region, locations and properties (such as the moments) of its corresponding region after motion are estimated using the coefficients computed using the Hough transform. These estimates are then used to find correspondences for all regions in a segment. Then, from the matches, the six motion parameters and the two structure parameters are found in closed form for a segment.

The basic formulation of the approach is described in the next section. Section 3 presents an algorithm. Experimental results and concluding remarks are presented in Section 4 and 5, respectively.

2 Mathematical formulation

In this section, we present the mathematical formulation of our approach. First we present the equations that are used to represent the displacement field induced by a rigid motion of a planar surface. Then we

*The support of Air Force Office of Scientific Research under grant AFOSR90-0061 is gratefully acknowledged.

TH0390-5/91/0000/0274/$01.00 © 1991 IEEE

describe how these equations are used to estimate motion and structure parameters from region correspondences.

2.1 Displacement field in the image plane

Let the right-handed coordinate system (X, Y, Z) be fixed on the camera with the origin coinciding with the projection center of the camera. X axis represents the vertical direction. Without loss of generality, we assume that the focal length is unity. Thus, the image plane is located at $z = 1$. Then, the perspective projection (x, y) on the image of a point (X, Y, Z) is given by

$$x = X/Z,$$
$$y = Y/Z.$$

Consider a point P on the object in 3D. Let $\vec{X} = (X, Y, Z)'$ be the 3D coordinate vector of P at time t_1 and let $\vec{X}' = (X', Y', Z')'$ be the corresponding vector at time t_2. Let $\vec{T}$ and $\mathbf{R}$ denote the translation vector and rotation about the unit axis $\vec{n} = (n_x, n_y, n_z)'$ by an angle θ, respectively. Then,

$$\vec{X}' = \mathbf{R}\vec{X} + \vec{T} \tag{1}$$

where

$$\mathbf{R} = \begin{bmatrix} r_{11} & r_{12} & r_{13} \\ r_{21} & r_{22} & r_{23} \\ r_{31} & r_{32} & r_{33} \end{bmatrix} \tag{2}$$

and

$$\vec{T} = [T_x T_y T_z]'.$$

Let (x, y) and (x', y') be the image coordinates corresponding to $\vec{X}$ and $\vec{X}'$, respectively. If the point P is on the plane $pX + qY + r = Z$ at time t_1, then

$$Z = \frac{r}{1 - px - qy}. \tag{3}$$

Hence, from Eqs.(1), (2) and (3),

$$x' = \frac{X'}{Z'} = \frac{a_1 + a_2 x + a_3 y}{a_7 + a_8 x + a_9 y} \tag{4}$$

$$y' = \frac{Y'}{Z'} = \frac{a_4 + a_5 x + a_6 y}{a_7 + a_8 x + a_9 y} \tag{5}$$

where

$$\left.\begin{array}{lll} a_1 = r_{13} + k_x & a_2 = r_{11} - pk_x & a_3 = r_{12} - qk_x \\ a_4 = r_{23} + k_y & a_5 = r_{21} - pk_y & a_6 = r_{22} - qk_y \\ a_7 = r_{33} + k_z & a_8 = r_{31} - pk_z & a_9 = r_{32} - qk_z \end{array}\right) \tag{6}$$

$$k_x \stackrel{\text{def}}{=} \frac{T_x}{r} \quad k_y \stackrel{\text{def}}{=} \frac{T_y}{r} \quad k_z \stackrel{\text{def}}{=} \frac{T_z}{r}. \tag{7}$$

Since the components of the translation in Eqs.(6) always appear normalized by the unknown r, therefore translation can only be determined up to the scale factor r. Further, the surface structure (represented here by p and q) can only be estimated if the translation is nonzero since p and q are eliminated in Eqs.(6) if $\vec{T} = \vec{0}$.

When θ is small , $\mathbf{R}$ can be approximated as follows:

$$\mathbf{R} = \begin{bmatrix} 1 & -w_z & w_y \\ w_z & 1 & -w_x \\ -w_y & w_x & 1 \end{bmatrix} \tag{8}$$

Then, the displacement vector (D_x, D_y) is represented by

$$D_x = x' - x = \frac{c_0 + c_1 x + c_2 y + c_3 xy + c_4 x^2}{a_7 + a_8 x + a_9 y} \tag{9}$$

$$D_y = y' - y = \frac{c_5 + c_6 x + c_7 y + c_4 xy + c_3 y^2}{a_7 + a_8 x + a_9 y} \tag{10}$$

where

$$\left.\begin{array}{ll} c_0 = k_x + w_y & c_1 = -pk_x - k_z \\ c_2 = -qk_x - w_z & c_3 = qk_z - w_x \\ c_4 = pk_z + w_y & c_5 = k_y - w_x \\ c_6 = -pky + w_z & c_7 = -qk_y - k_z \end{array}\right). \tag{11}$$

Using Eqs.(3), (6) and (7), the denominator in Eqs.(9) and (10) can be rewritten as follows:

$$a_7 + a_8 x + a_9 y = 1 + \frac{T_z}{Z} + (-w_y x + w_x y).$$

The second term in the above equation can be ignored if the translation in the Z direction is small relative to the object distance from the camera and the third term can be ignored if the rotation angle and the image plane coordinates are small. Hence, if we assume that (1) $\frac{T_z}{Z} \ll 1$, (2) the field of view of the camera is small, and (3) the rotation angle is small, then

$$a_7 + a_8 x + a_9 y \approx 1.$$

These assumptions which are quite common in motion analysis are not very restrictive since the field of view of a camera is small in practice and the amount of motion is small if the time interval between two images is short. As in [4], we will approximate the displacement vector by the second order polynomials in (x, y). Note that we are approximating the displacements D_x and D_y instead of x' and y' since $| D_x |$ and $| D_y |$ are usually smaller than $| x' |$ and $| y' |$, respectively.

$$D_x = x' - x = c_0 + c_1 x + c_2 y + c_3 xy + c_4 x^2 \tag{12}$$

$$D_y = y' - y = c_5 + c_6 x + c_7 y + c_4 xy + c_3 y^2. \tag{13}$$

The next step is to find the eight unknowns $c_0 \ldots c_7$ in Eqs.(12) and (13) from region correspondences and then to get motion and structure parameters from them. Although the eight unknowns can be easily computed if a sufficient number of point correspondences are given, we use region correspondences for this purpose instead of point correspondences for reasons stated in Section 1.

2.2 Motion and structure estimation from region correspondences

Now, we would like to relate region properties to 3D motion and structure. Eqs.(12) and (13) define a mapping $G : (x, y) \rightarrow (x', y')$. Hence,

$$G(x, y) \stackrel{\text{def}}{=} (g_1(x, y), g_2(x, y)) = (x', y') = (x+D_x, y+D_y).$$

Let M and N be the corresponding regions at two time instants. For a smooth function f, we know

$$\int\int_N f(x, y)dxdy = \int\int_M f(x + D_x, y + D_y)Jdxdy \tag{14}$$

where J is the Jacobian:

$$J = \left| \frac{\partial g_1}{\partial x}\frac{\partial g_2}{\partial y} - \frac{\partial g_1}{\partial y}\frac{\partial g_2}{\partial x} \right|. \tag{15}$$

Using Eqs.(4), (5), (6) and (15), we get

$$J = \frac{| -a_2a_4a_9 + a_2a_6a_7 - a_1a_6a_8 - a_3a_5a_7 + a_3a_4a_8 + a_1a_5a_9 |}{| (a_7 + a_8x + a_9y)^3 |} \tag{16}$$

The numerator of J in Eq.(16) is a constant and the expression in the denominator can be rewritten as in Section 2.1.1:

$$a_7 + a_8x + a_9y = 1 + \frac{T_z}{Z} + (-w_yx + w_xy).$$

We assume that the three conditions stated in Section 2.1.1 are satisfied. Then, the second and third terms are small compared to 1. Further, variations in Z, x and y is not large since the integration is performed over the region M in the image plane which is small. Hence, the denominator of J can be approximated as a constant over M. Then, Eq.(14) becomes,

$$\int\int_N f(x, y)dxdy \approx J\int\int_M f(x + D_x, y + D_y)dxdy. \tag{17}$$

Note that if $f = 1$, then the equation just represents the area relationship.

$$N_{00} = JM_{00} \tag{18}$$

where

$$N_{ij} \stackrel{\text{def}}{=} \int\int_N x^i y^j dxdy$$
$$M_{ij} \stackrel{\text{def}}{=} \int\int_M x^i y^j dxdy. \tag{19}$$

Hence, given a pair of regions at two time instants, J can be treated as a constant which can be easily computed. In principle, we can use a sufficiently large number of functions f to get the eight unknowns $c_0 \ldots c_7$. However, we use only two functions $f = x$ and $f = y$ since these choices make $f(x+D_x, y+D_y)$ linear in coefficients $c_0 \ldots c_7$. Hence, by Eqs.(12), (13), (17) and (18), we get two equations for each region correspondence.

$$\frac{N_{10}}{N_{00}} - \frac{M_{10}}{M_{00}} = c_0 + c_1\frac{M_{10}}{M_{00}} + c_2\frac{M_{01}}{M_{00}} + c_3\frac{M_{11}}{M_{00}} + c_4\frac{M_{20}}{M_{00}} \tag{20}$$

$$\frac{N_{01}}{N_{00}} - \frac{M_{01}}{M_{00}} = c_5 + c_6\frac{M_{10}}{M_{00}} + c_7\frac{M_{01}}{M_{00}} + c_4\frac{M_{11}}{M_{00}} + c_3\frac{M_{02}}{M_{00}}. \tag{21}$$

Eqs.(20) and (21) represent the constraints from which the motion and structure parameters are to be estimated using a sufficiently large number of region correspondences. Therefore, the coefficients $c_0 \ldots c_7$ can be computed from four or more region correspondences.

3 Algorithm

The input to our algorithm is regions detected in the two images. The algorithm first groups regions based on the similarity of six first order flow coefficients $c_0, c_1, c_2, c_5, c_6, c_7$, thus segmenting the image using a coarse first order displacement model. This step also establishes the correspondences between regions in the two images. Regions in a group have similar values of their coefficients and represent the same planar surface. The flow coefficients of different groups are different and they represent different planes. For each group of regions, the motion and structure are characterized more accurately by invoking the original second order displacement model. All eight coefficients $c_0 \ldots c_7$ are now computed using identified region correspondences and least squares estimation. Motion and structure parameters of each segment then follow in closed form from the known values of the eight coefficients. These two steps will be explained in more detail in the following subsections.

3.1 Segmentation and matching

We assume that each distinct segment of regions (having distinct motion or structure properties) can be differentiated by the first order approximation. Thus, if we neglect the second order coefficients c_3 and c_4 in Eqs. (12) and (13), then

$$D_x = c_0 + c_1x + c_2y \tag{22}$$
$$D_y = c_5 + c_6x + c_7y. \tag{23}$$

For a smooth function f, we get

$$\int\int_N f(x, y)dxdy = \int\int_M f(x + D_x, y + D_y)J'dxdy \tag{24}$$

where

$$J' = \left| (c_1 + 1)(c_7 + 1) - c_2c_6 \right|. \tag{25}$$

Again, for $f = x$ and $f = y$, we get two equations for each region correspondence.

$$\frac{N_{10}}{J'} - M_{10} = c_0M_{00} + c_1M_{10} + c_2M_{01}$$

$$\frac{N_{01}}{J'} - M_{01} = c_5M_{00} + c_6M_{10} + c_7M_{01}$$

where

$$J' = \frac{N_{00}}{M_{00}},$$

and, $N_{10} \ldots M_{01}$ are defined in the same way as in Eqs.(19). These can be rewritten as follows:

$$C'_x = c_0 + (1 + c_1)C_x + c_2 C_y \quad (26)$$

$$C'_y = c_5 + c_6 C_x + (1 + c_7)C_y \quad (27)$$

where

$$C'_x = \frac{N_{10}}{N_{00}} \quad C'_y = \frac{N_{01}}{N_{00}}$$

$$C_x = \frac{M_{10}}{M_{00}} \quad C_y = \frac{M_{01}}{M_{00}}.$$

We see that these are the relationships of the 2D coordinates of the centroids of the corresponding regions. To group the regions which satisfy the same affine transformation of centroids, the generalized Hough transform is used [4, 7]. Each point in the discrete multidimensional parameter space $(c_0, c_1, c_2, c_5, c_6, c_7)$ uniquely defines a transformation. The segmentation and matching consists of two steps. First, for each region M in the first image, the regions in the second image whose centroids are within a predetermined distance l from the centroid of M vote for each point in the 6D parameter space $(c_0, c_1, c_2, c_5, c_6, c_7)$ if the constraints on centroids (Eqs.(26) and(27)) are satisfied. The value of l used determines the extent of motion allowed between successive images. The larger the allowed value of l, the larger the computation complexity. In our experiments, $l = 125$ pixels is used. The part of the parameter space that accumulates the greatest density of votes corresponds to the most dominant motion and structure parameters. The second step is to find the corresponding region in the second image for each region in the first image by using the set of six parameters which has the largest votes in step 1. Only regions within the distance l in the second image from a region in the first image are considered. A region N in the second image is matched to the region M in the first image if the two regions satisfy Eqs.(26) and (27) and the following Jacobian constraint on the area:

$$J = \frac{N_{00}}{M_{00}} = \mid (1 + c_1)(1 + c7) - c_2 c_6 \mid . \quad (28)$$

The execution of the above two steps establishes correspondences for the regions in the segment having the largest number of regions in it (corresponding to the tallest peak in the Hough space). Next, these regions are deleted from consideration, the Hough transform is recomputed, and the correspondences are found for the regions in the next largest segment. This process continues until all image regions are matched.

In this way, grouping and matching are done simultaneously. In particular, regions are matched based on the constraints on physically feasible motion. If region matching is attempted based solely on 2D attributes and relative 2D locations, it may fail, for example, near the image boundary, where relative region locations are not stable, or for motion along the optical axis which involves significant change in 2D properties of the regions.

3.2 Closed-form estimation of motion and structure parameters

After segmentation and matching, for each group of regions which are estimated to be on the same planar surface, we linearly compute all eight coefficients $c_0 \ldots c_7$ from Eqs.(20) and (21) by least squares method, provided the number of regions available is at least four. After $c_0 \ldots c_7$ are found, 8 unknowns $(p, q, k_x, k_y, k_z, w_x, w_y, w_z)$ are computed from the eight equations in Eqs.(11) in closed form using the algebraic method in [6]. (They showed the k_z is uniquely determined from the eight coefficients $c_0 \ldots c_7$ and there are dual solutions associated with each possible k_z.) Then, $\vec{n}$ and θ are found from (w_x, w_y, w_z) in a straightforward way.

4 Implementation and experimental results

4.1 Implementation details

In the first step of the segmentation and matching, the range of each of the six parameters $(c_0, c_1, c_2, c_5, , c_6, c_7)$ is taken to be from -128 pixels to 128 pixels with increments of 0.5 pixel. This yields to 512^6 points which is large. We use two methods to reduce computational complexity, as in [4]. First, search over the parameter space is performed at multiple resolutions. Secondly, we decompose the parameter set into two disjoint subsets (c_0, c_1, c_2) and (c_5, c_6, c_7). The Hough method is separately applied to the corresponding 3D parameter spaces, using Eqs.(26) and (27), respectively.

We use three resolutions for coarse-to-fine search of each of the two spaces (c_0, c_1, c_2) and (c_5, c_6, c_7). At a coarse resolution, candidates of points which have the largest supports in 3D parameter space are found. Then, the parameter space is quantized by $8 \times 8 \times 8$ around each candidate point, and new candidate points which represent more accurate values are obtained. Then, combination of solution triples is obtained which best satisfies Eqs.(26) and (27). This usually gave the maxima in 6D parameter space.

4.2 Experiments

Experiments with three different image pairs were conducted. The first image in each experiment shows a real image. The second image is generated from the first image by simulated motion, but the coordinates are rounded off to integers to simulate quantization noise. From the original intensity image, edges are detected using the Laplacian of Gaussian operator $(\nabla^2 G)$. These stages also introduce some noise. Then regions are extracted using an algorithm described in [8]. After regions are detected in images at both time instants, our algorithm is applied. Units for translation and rotation angle are in meters and radians, respectively. Note that r in Eq.(3) cannot be determined since we are using the monocular images.

4.2.1 Experiment 1

The first experiment simulates a general motion, represented by $\vec{T} = (-0.01, 0.01, 0.06)'$ and $\vec{n} = (1, 0, 0)'$ with angle $\theta = 0.01$. The scene has only one surface with $(p, q, r) = (0, 1, 1)$. Focal length is 35mm and the field of view of the camera is approximately 13 degrees. Fig 1 shows the first image and the matching result. The matching results are error free and only one segment (plane) is found as expected. The dual solutions are as follows:

Solution 1:

$p = 0.053$ $q = 0.939$ $\vec{T} = (-0.01, 0.009, 0.057)'$
$\theta = 0.009$ $\vec{n} = (.996, 0.071, 0.045)'$

Solution 2:

$p = 0.176$ $q = -0.163$ $\vec{T} = (-0.003, -0.054, 0.057)'$
$\theta = 0.055$ $\vec{n} = (-0.978, -0.116, -0.174)'$

We see that solution 1 is in good agreement with the actual values. Note that for the given images, it is very hard to precisely locate point features and to find point correspondences, hence techniques based on the points will have greater difficulty.

4.2.2 Experiment 2

In this experiment, there are two planes in the scene, which are two sides of a box. The motion of the camera with respect to the scene is represented by $\vec{T} = (0.04, -0.04, 0.05)'$ and $\vec{n} = (1, 0, 0)'$ with angle $\theta = 0$. The left planar surface has $(p, q, r) = (0, -1, 1)$, while the right one has $(p, q, r) = (0, 1, 1)$. Focal length used is 20mm and the field of view of the camera is approximately 22 degrees. The first frame and the matching result are shown in Fig 2. The regions are matched without any error and two segments (planes) were found as expected. The dual solutions of each plane are as follows:

Right Plane

Solution 1 :

$p = 0.233$ $q = 0.959$ $\vec{T} = (0.047, -0.033, 0.035)'$
$\theta = 0.013$ $\vec{n} = (.435, -0.684, -0.586)'$

Solution 2:

$p = -1.324$ $q = -0.924$ $\vec{T} = (-0.008, -0.034, 0.035)'$
$\theta = 0.065$ $\vec{n} = (0.067, 0.716, 0.695)'$

Left Plane

Solution 1 :

$p = -0.123$ $q = -0.889$ $\vec{T} = (0.043, -0.036, 0.053)'$
$\theta = 0.006$ $\vec{n} = (0.271, -0.768, 0.581)'$

Solution 2:

$p = -0.801$ $q = 0.683$ $\vec{T} = (0.007, 0.047, 0.053)'$
$\theta = 0.099$ $\vec{n} = (0.863, 0.317, -0.393)'$

Solution 1 of each plane is in good agreement with the actual values. The sources of errors include quantization noise, small number of regions, and distortion due to $\nabla^2 G$. In this case, we can iteratively improve a solution by using the fact that two surfaces of a rigid object have the same motion.

4.2.3 Experiment 3

This third experiment uses images that simulate motion over Champaign County. The first image is a real aerial view, and shows a big, approximately planar surface. The parameters of simulated motion are $\vec{T} = (0.01, -0.02, 0.01)'$ and $\vec{n} = (-0.577, -0.577, -0.577)'$ with angle $\theta = 0.02$. The whole planar surface has $(p, q, r) = (0.5, 0, 1)$. Focal length is 17.5mm and the field of view of the camera is approximately 25 degrees. The images, detected regions, and the matching results are shown in Fig 3. The regions are correctly matched and one segment (plane) is found as expected. The dual solutions of the plane are as follows:

Solution 1 :

$p = 0.601$ $q = -0.068$ $\vec{T} = (0.01, -0.016, 0.008)'$
$\theta = 0.017$ $\vec{n} = (-0.432, -0.657, -0.617)'$

Solution 2:

$p = -1.209$ $q = 1.90$ $\vec{T} = (-0.005, 0.001, 0.008)'$
$\theta = 0.01$ $\vec{n} = (0.909, 0.364, -0.204)'$

The result (Solution 1) is better compared to Experiments 1 and 2 since there are many regions available in the scene.

5 Concluding Remarks

We have presented an algorithm which segments and matches the regions and then estimates non-iteratively motion and structure of piecewise planar surfaces. This method is useful especially when features like points or lines are not available as is the case, for example, in Fig 1.

The advantage of our algorithm is that it is less sensitive to noise than the point-based methods because it uses regions as features which are more robust features than points. Further, we can find corresponding regions very reliably and this makes it easier to find point correspondence.

References

[1] K. Kanatani, "Detecting the motion of a planar surface by line and surface integrals," *Computer Vision, Graphics, and Image Processing*, vol.29,1985, pp.13-22

[2] K. Kanatani and T. Chou, "Tracing finite motions without correspondence," in *Proc of Image Understanding Workshop*, DARPA, Feb., 1987, pp.704-718

[3] J. Wu, R. Brockett and K. Wohn, "A contour-based recovery of image flow: Iterative method," in *Proc. IEEE Conf. Computer Vision and Pattern Recognition*, San Diego, CA, 1989, pp124-129

[4] G. Adiv, "Determining three-dimensional motion and structure from optical flow generated by several moving objects," *IEEE Trans. Pattern Anal. Machine Intell.*, vol.PAMI-7, no.4, July, 1985

[5] G. Adiv, "Inherent ambiguities in recovering 3-D motion and structure from a noisy flow field," *IEEE Trans. Pattern Anal. Machine Intell.*, vol.PAMI-11, no.5, pp.477-489, May, 1989

[6] M. Subbarao and A. Waxman, "Closed form solutions to image flow equations for planar surfaces in motion," *Computer Vision, Graphics, and Image Processing*, vol.36,1986, pp.208-228

[7] J. O'Rourke, "Motion detection using Hough techniques," in *Proc. IEEE Conf. Pattern Recog. Image Proc.*, Dallas, TX, 1981, pp82-87

[8] V. V. Swaminathan and N. Ahuja, "Multiresolution region detection," unpublished manuscript

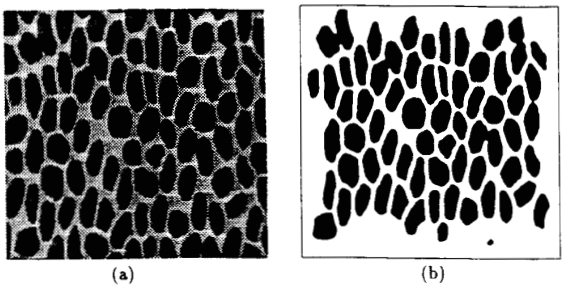

(a) (b)

Figure 1: Experiment 1. (a)The first image. (b)Matched and segmented regions in the first image.

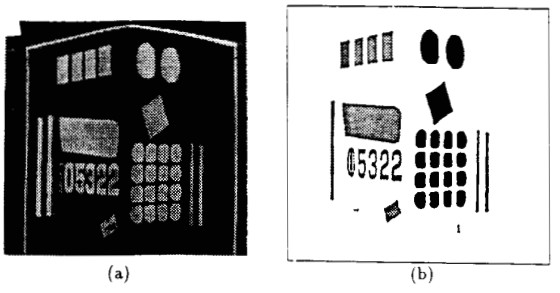

(a) (b)

Figure 2: Experiment 2. (a)The first image. (b)Matched and segmented regions in the first image. Note that the segmented two planes are illustrated using two different intensity values.

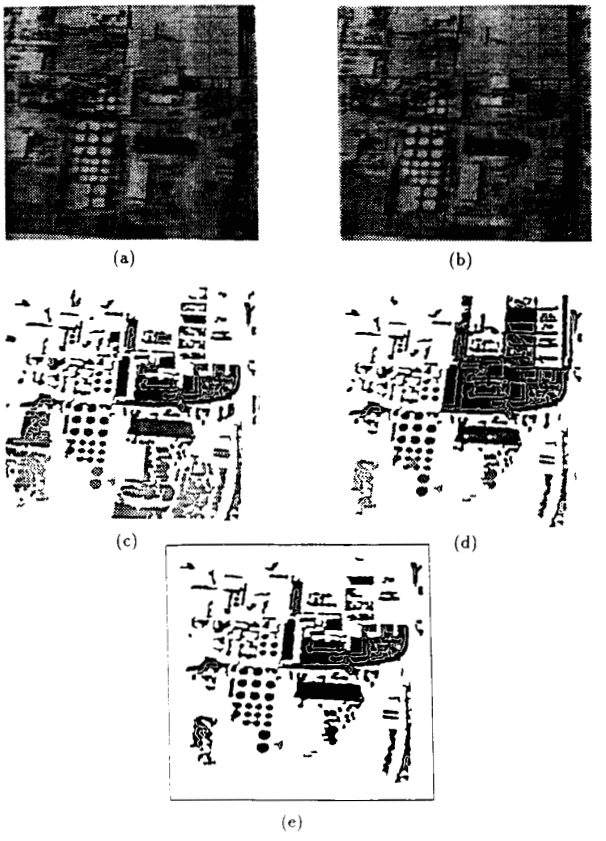

(a) (b) (c) (d) (e)

Figure 3: Experiment 3. (a)The first image. (b)The second image. (c)Detected regions in the first image. (d)Detected regions in the second image. (e)Matched and segmented regions in the first image.